

Research report

# Organization of the circadian system in the subterranean mole rat, *Cryptomys hottentotus* (Bathyergidae)

Julia Negroni<sup>a,c,\*</sup>, Nickel C. Bennett<sup>b</sup>, Howard M. Cooper<sup>a</sup>

<sup>a</sup>INSERM Unité 371, 'Cerveau et Vision', 18 Avenue du Doyen Lépine, 69675 Bron, France

<sup>b</sup>Department of Zoology and Entomology, University of Pretoria, Pretoria, South Africa

<sup>c</sup>CNRS UMR 7593 'Vulnérabilité, Adaptation et Psychopathologie' Université Paris VI, 91 Bd de l'Hôpital, 75013 Paris, France

Accepted 11 December 2002

## Abstract

The mole rat, *Cryptomys hottentotus* (Bathyergidae) is a gregarious subterranean rodent, which shows no entrainment to ambient light–dark cycles. The locomotor activity of individuals or of a whole colony, which shows no circadian rhythmicity. Since the lack of both synchronization to light–dark cycle and an endogenous rhythm of locomotor activity could be related to the organization of the circadian system, we have investigated the neuropeptidergic features of the SCN and IGL, and have used pseudorabies viral tracing methods to identify the visual and circadian pathways in this species. The precise topographic distribution of certain neuropeptide populations in the SCN differs from typical rodent pattern of organization and may be correlated with the apparent absence of light entrainment of activity and lack of endogenous rhythmicity. The IGL is highly reduced in size. This structure can nevertheless be identified by the presence of NPY and CALB positive neurons, as well as by a dense network of SP fibers. Viral tracing using intraocular injection of the PRV-Becker and PRV-Bartha strains, leads to differential infection of neurons in circadian and visual structures. With the Bartha strain, infected neurons are principally observed in the SCN, whereas the Becker strain leads primarily to infection of the dLGN and shows an anatomical regression of visual structures. Transsynaptic retrograde infection of the retina contralateral to the injected eye reveals a morphologically homogeneous population, which resemble to retinohypothalamic ganglion cells described in other mammals. © 2002 Elsevier Science B.V. All rights reserved.

**Theme:** Other systems of the CNS

**Topic:** Comparative neuroanatomy

**Keywords:** Social subterranean rodent; Suprachiasmatic nucleus; Intergeniculate leaflet; Neurotransmitters; Transneuronal viral tracing technique; Retina

## 1. Introduction

The mole rat, *Cryptomys hottentotus* (Bathyergidae), is a social, subterranean rodent living in colonies of 4–18 individuals in semi-arid regions of South Africa [4]. Most

studies of the visual system have been limited to descriptions of the general morphology of the eye. In *Cryptomys* the eye measures 2.1 mm in diameter and is embedded in a large Harderian gland. Extraocular eye muscles are degenerate and a pupillary reflex is absent [21]. The retina appears relatively normal in structure and contains all nuclear and plexiform layers, with a sparse population of ganglion cells. The optic nerve is thin and is mainly composed of unmyelinated fibers [18].

Behavioral studies have shown that *Cryptomys* do not seem to react to light. For example, a flash of light elicits no overt reaction, and attempts to obtain a conditioned response of the animal to a light combined with a puff of air were unsuccessful [21]. More recent studies have shown that colonies of *Cryptomys* show no distinct rhythmic locomotor activity, and individual patterns of

**Abbreviations:** CALB, calbindin; CT–HRP, cholera toxin–horseradish peroxidase; GRP, gastrin releasing peptide; dLGN, dorsal lateral geniculate nucleus; ENK, enkephalin; IGL, intergeniculate leaflet; NPY, neuropeptide Y; OT, optic tract; PARV, parvalbumin; PRT, pretectum; PRV, pseudorabies virus; RGC, retinal ganglion cells; SC, superior colliculus; SCN, suprachiasmatic nucleus; SP, substance P; VIP, vasoactive intestinal polypeptide; vLGN, ventral lateral geniculate nucleus; VP, vasopressin. III, third ventricle; 5-HT, serotonin

\*Corresponding author. Tel.: +33-140-779-705; fax: +33-153-790-770.

E-mail address: [negroni@ext.jussieu.fr](mailto:negroni@ext.jussieu.fr) (J. Negroni).

behavior are not synchronized to the daily light cycle [5,24]. These observations are in contrast with studies of the blind mole rat, *Spalax*, which have demonstrated light entrainment of an endogenous circadian rhythm despite the minute subcutaneous eye [52,53,63]. In *Spalax*, as in other rodents, light induced fos expression in the SCN is restricted to the subjective night-time period [63,66]. Apart from *Spalax*, in which the eye, retinal pathways [7,17,18] and neuroanatomical organization of the SCN [44] have been described in detail, few studies of the organization of the circadian system of subterranean mammals are available [32] and no study has dealt with social species such as *Cryptomys*.

Since *Cryptomys* appears to lack both an endogenous rhythm and light entrainment of locomotor activity, we have investigated the organization of the visual and circadian system using immunohistochemical and viral tracing techniques. One objective is to characterize the neurotransmitters of the two main retinorecipient structures of the circadian system, the suprachiasmatic nucleus (SCN) and the intergeniculate leaflet (IGL). The SCN and IGL contain characteristic neurotransmitters and connections, which are involved in the generation and regulation of the endogenous circadian rhythm, and which have been demonstrated in rodents (mouse [13,16]; hamster [42]; *Spalax* [44]; rat [65]) and in other species (cat [13]; primate [39]; sheep [62]). For example, vasoactive intestinal peptide (VIP) in the SCN shows quantitative variations, which are modulated by the external light cycle [55], whereas the levels of vasopressin (VP) show endogenous variation in constant conditions [30]. Afferent projections to the SCN from the raphe nucleus, containing 5-HT, or from the IGL, containing neuropeptide Y, also mediate the activity of the SCN [10].

A second objective is to determine the relative degree of development of the visual perceptual and circadian components of the visual system using a viral tracing technique which employs different strains of a pseudorabies virus, 'PRV'; type 1 alpha-herpes porcine virus [11]. Two strains of PRV show selective neurotropic properties in the central and peripheral nervous system [12,59]. Following an intraocular injection, the wild type PRV-Becker strain [3] infects all retinal ganglion cells (RGC), and is anterogradely transported in RGC axons to target neurons in visual structures. An initial wave of infection (from 70–90 h depending on the species) will lead to labeled neurons in visual structures of the thalamus (ventral and dorsal lateral geniculate nucleus, pretectum) and mesencephalon (superior colliculus, accessory optic system). Structures of the circadian system, including the SCN and the IGL, contain infected neurons during a lagged, second wave, occurring with a delay 24 h later. In contrast, the attenuated PRV-Bartha strain [2] will preferentially infect neurons in the SCN and the IGL, in temporal correspondence with the second wave of infection by the PRV-Becker strain. The limited infection in retinorecipient structures after in-

travitreal application of PRV Bartha has been interpreted as a restricted tropism of PRV Bartha for a subset of retinal ganglion cells [11]. Recently, further works called this interpretation into question. Indeed, genetic analysis indicated that PRV Bartha might be incapable of anterograde spread through chains of connected neurons [6,27,64]. Pickard et al. showed that the infection of retinorecipient structures such as the SCN and IGL after intravitreal PRV Bartha injection results from retrograde transsynaptic transport via autonomic afferents to the eye and not by anterograde transport via the optic nerve [50].

Consequently, the viral tracing technique provides two advantages. First, following the initial infection and transsynaptic passage into the target neuron, the intracellular replication of the virions, allows an amplification of the signal, and thus a high sensitivity of detection [33]. A second advantage is that after the replication in the target cell, the virus is retrogradely and transsynaptically transported to afferent neurons, allowing demonstration of synaptically linked chains of neurons. Since this technique has been used for to identify the ganglion cells afferent to retinorecipient structures in several rodents [41,51], we have also applied this approach in our study of *Cryptomys*, using the PRV-Bartha strain.

## 2. Materials and methods

The experiments were performed in accordance with the European Communities Council Directive of 24 November 1986 (86/609/EEC).

### 2.1. Immunohistochemistry of the SCN and IGL

The animals used in this study are the species *Cryptomys hottentotus pretorii* from the northern region of South Africa. Eight adult animals (4 males and 4 females) were used for the immunohistochemical and cytoarchitectural studies. Animals were anesthetized with a lethal injection of sodium pentobarbital and perfused with a warm (37 °C) saline solution (0.9% NaCl, 0.1% procaine) followed by Zamboni's fixative [68]. The brains were removed and sunk overnight in a 30% sucrose solution in phosphate buffer (pH 7.4, 0.1 M). The brains were then sectioned at 40 µm on a freezing microtome and collected in phosphate buffer.

For immunohistochemistry, endogenous peroxidase was first suppressed using a solution of 50% ethanol alcohol in 0.9% NaCl with 0.05% H<sub>2</sub>O<sub>2</sub> for 30 min. All procedures were carried out at 4 °C with agitation (unless specified otherwise). Sections were then rinsed in phosphate buffer (pH 7.4, 0.1 M) containing 0.3% Triton X100, 0.1% sodium azide, and 0.9% NaCl (PBSTA). Non-specific sites were saturated with a 1.5% solution of normal serum (goat, S-1000 or horse, S-2000 according to the primary antibody host, Vector Laboratories, Burlingame, CA, USA)

in PBSTA during 1 h. Sections were rinsed in PBSTA and incubated for 72 h in the primary antibody diluted in PBSTA and 1.0% normal serum. After incubation, sections were rinsed twice in PBST and then incubated for 2 h (room temperature) in a secondary biotinylated antibody (anti-rabbit Ba-1000 or anti-mouse Ba-2000 IgG, Vector Laboratories, Burlingame, CA, USA), diluted 1/200 with 1.0% normal serum. After 2 rinses in PBST, immunoreactivity was visualized using a Vectastain ABC Elite Kit (PK-6100, Vector Laboratories, Burlingame, CA, USA), followed by incubation in 0.02% 3,3-diaminobenzidine (Sigma, St. Quentin Fallavier, France) with 0.5% ammonium nickel sulfate and 0.001% H<sub>2</sub>O<sub>2</sub> in Tris buffer for 5–20 min depending on the intensity of label. Sections were rinsed in Tris and then mounted on gelatinized slides, and coverslipped with Depex.

The primary antibodies and the dilutions used included vasopressin (1/5000), neuropeptide Y (1/5000), serotonin (1/30 000), gastrin releasing peptide (1/2000), substance P (1/20 000); the calcium binding proteins calbindin (1/1000) and parvalbumin (1/2500; both from Sigma, St Louis, CA, USA), L-enkephalin 1/5000 (INRA, Nouzilly, France), and vasoactive intestinal polypeptide (1/1000; generously provided by Möller, Copenhagen, Denmark [38]). Brain sections were divided into 2 or 3 alternate series for incubation in different antibodies: VP/5-HT/VIP ( $n=2$ ), NPY/GRP ( $n=2$ ), SP/PARV/CALB ( $n=1$ ) and L-ENK/SP ( $n=1$ ). The specificity of the antibodies was tested by replacing the primary or secondary antibodies with normal serum at the same concentration as the antibody. No labeling was observed in control sections. Two series of brain sections ( $n=2$ ) were also stained with cresyl violet for cytoarchitectural identification of the SCN and IGL.

### 2.2. CT–HRP Intraocular Injections and histological treatment

Two adults *Cryptomys hottentotus* (2 males) received an intraocular injection of 2–3  $\mu$ l of 0.2% cholera toxin subunit B conjugated with horseradish peroxidase (CT–HRP, List Biological laboratories) using a glass pipette (50 ml tip) sealed to the needle of a 10  $\mu$ l Hamilton syringe. The animals survived for periods of 48–72 h before perfusion. For fixation, animals received a lethal dose of sodium pentobarbitol and were perfused through the heart with 100 ml of warm saline (0.9%) followed by 400 ml of cold 4% paraformaldehyde in phosphate buffer (0.1 M, pH 7.4). This was followed by a post-fixation rinse of 10% sucrose in same buffer. The brain was removed and stored in 30% buffered sucrose at 4 °C prior to sectioning. For CT–HRP histochemistry, the brains were sectioned on a freezing microtome in the coronal plane at a thickness of 30  $\mu$ m. The sections were reacted using 3,3',5,5'-tetramethylbenzidine (Sigma, St Quentin Fallavier, France) as a chromagen, according to the method of Mesulam [37] as

modified by Gibson et al. [22]. Sections were mounted on gelatinized slides and allowed to dry overnight, dehydrated and cleared in xylene coverslipping with depex.

### 2.3. Tracing experiments using pseudorabies virus

The pseudorabies virus was cultivated in porcine fibroblasts (PK15) at the neuroscience laboratory (provided by P. Card, University of Pittsburg, CA, USA). Infected cells were collected, sonicated, centrifuged and the supernatant stored at –80 °C. The titration of plaque forming units (pfu) used in our experiments were  $6 \times 10^8$  pfu/ml for the Becker strain, and  $5 \times 10^8$  pfu/ml for the Bartha strain.

Nine adults *Cryptomys hottentotus* (5 males and 4 females) received intraocular injections. The animals were anesthetized with an intramuscular injection of ketamine hydrochloride (60 mg/kg,) and xylazine (7 mg/kg,). The virus was unfrozen, maintained on ice and each animal received an intraocular injection into the vitreous chamber of 1.0–1.5  $\mu$ l solution containing the PRV-Bartha or the PRV-Becker strain. The injection was made using a micropipette (50  $\mu$ m diameter tip) sealed to the needle of a 5  $\mu$ l Hamilton syringe. Survival times ranged from 66 to 90 h with the Becker strain, and from 70 to 118 h with the Bartha strain. For each survival time, only one animal was used. Two survival times (81 and 90 h) were not analyzed in the present study. Indeed, animals infected with the wild type Becher did not survive longer than 82 h and no infected neuron was observed in any region of central nervous system after 81 h survival with the Bartha strain.

For the immunohistochemical demonstration of the virus, the anesthesia, perfusion, and sectioning of the animals was performed as described above. The immunohistochemical technique using DAB as the chromagen was also identical to that described above, except for the primary anti-PRV antibody raised in rabbit and used at 1/10 000 dilution (Rb-133, generously supplied by P. Card, University of Pittsburg, CA, USA [11]). All the brain sections, from the preoptic region to the posterior pole of the superior colliculus were examined.

In certain cases the retinas contralateral to the injected eye were flat mounted to examine the retinal ganglion cells infected by the PRV-Bartha strain following transsynaptic transport. The eyes were cut at the level of the ora serrata and the retina removed whole, with the dorsal axis of the optic globe marked for orientation. Immunohistochemistry for demonstration of the virus was performed using the anti-PRV antibody, after which the retinas were placed ganglion cell layer upwards on a gelatinized slide. Due to the small size and fragility of the retina, successive dehydrations in alcohol and clearing in xylene were done by gently maintaining the retina between the slide and a coverslip, while changing the various solutions. After the final passage in xylene, the retina was coverslipped with Depex.

Cell counts and quantitative morphology of labeled virally infected cells in the brain and the retina were performed using computer assisted image analysis coupled to the microscope (Biocom, Les Ulis, France). The total number of infected neurons has to be given from one animal at each survival time.

### 3. Results

#### 3.1. Suprachiasmatic nucleus

In cresyl violet stained coronal sections, the SCN in *Cryptomys* is a distinct structure of the rostral hypothalamus (Fig. 1A). As in other mammals, the SCN is a paired structure located dorsal to the optic chiasm, on each side of the third ventricle. The nucleus is pyriform in

shape. The ventral and ventromedial region of the SCN contains mainly small, densely stained, and tightly packed cells, whereas in the dorsal region, larger less densely stained cells predominate. Retinal afferents to the SCN are demonstrated by anterograde transport of CT–HRP (Fig. 1B). In CT–HRP stained coronal sections, the SCN in *Cryptomys* receives bilateral retinal afferents with a predominance on the ipsilateral side to the injected eye. The greatest density of retinal afferents is observed in the medial and ventro–medial regions.

##### 3.1.1. Vasoactive intestinal polypeptide (VIP)

Cells containing VIP are located in the ventral region of the SCN (Fig. 1C). Many fine diameter VIP fibers extend to fill the entire dorsal region of the SCN. Other regions of the hypothalamus are devoid of VIP positive cells or fibers.

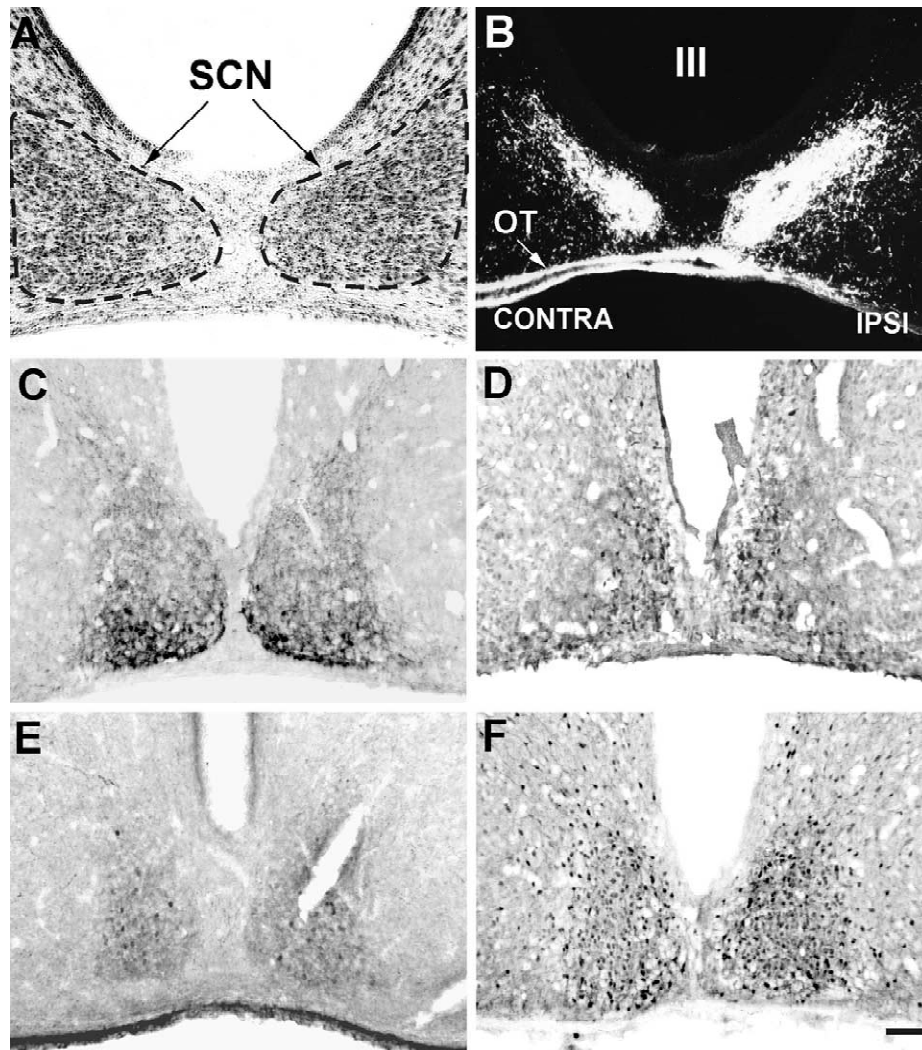


Fig. 1. Organization of the suprachiasmatic nucleus (SCN) in *Cryptomys*. (A) Shows the cytoarchitecture of the nucleus in a cresyl violet stained, coronal section and (B) retinal afferents demonstrated by intraocular injection of CT–HRP. The distribution of immunopositively stained neurons to different neuropeptides is shown in (C): Vasoactive intestinal polypeptide, (D): Vasopressin, (E): Gastrin releasing peptide, and in (F): To the calcium binding protein, calbindin. OT, optic tract; III, third ventricle. Scale: 100  $\mu$ m.

### 3.1.2. Vasopressin (VP)

VP immunopositive cells are located in the ventral and medial regions of the nucleus with the medial cells extending up towards the dorsal region, forming a crescent shaped distribution (Fig. 1D). VP immunopositive cells are also evident in other regions of the hypothalamus, including the anterior hypothalamus, the supraoptic nucleus and the paraventricular nucleus. The two latter structures are linked by a distinct bundle of VP positive fibers.

### 3.1.3. Gastrin releasing peptide (GRP)

Cells and fibers containing GRP are distributed in the ventral and central regions of the SCN (Fig. 1E). This distribution partly overlaps with that of VIP and VP containing neurons, and NPY fibers. Fibers immunopositive to GRP in the SCN are sparse, and in other regions of the hypothalamus both GRP positive cells and fibers are absent.

### 3.1.4. Calbindin (CAL)

Neurons containing this calcium binding protein show a uniform and dense distribution throughout the entire nucleus (Fig. 1F). In coronal section, the peripheral border of the SCN is devoid of CALB containing neurons. CALB containing neurons are abundant in the entire anterior region of the hypothalamus, as well as in the paraventricular nucleus.

### 3.1.5. Neuropeptide Y (NPY)

NPY immunopositive fibers are distributed in the lateral and ventral regions of the SCN, forming a crescent, which is partly complementary to the distribution of VP containing cells (Fig. 2A). The greatest density is observed in the ventral region, and fibers tend to avoid the central and dorsal regions of the nucleus. NPY fibers are also observed surrounding the third ventricle, in the anterior hypothalamus, and in the thalamic and hypothalamic paraventricular nuclei.

### 3.1.6. Serotonin (5-HT)

Fibers containing 5-HT form a dense plexus in the SCN (Fig. 2B). Rostrally these fibers are located in the ventral region, and only partially overlap with the distribution of VIP neurons, in part with VP neurons, but not with NPY fibers. Towards the caudal pole of the nucleus, 5-HT fibers are restricted to the medial region of the SCN. Immunopositive fibers avoid the lateral and central regions of the nucleus. Although the periphery of the SCN is relatively devoid of 5-HT fibers, the remainder of the hypothalamus is filled with a light mesh of immunopositive fibers, and in particular the hypothalamic and thalamic paraventricular nuclei.

### 3.1.7. Substance P (SP)

The SCN is completely devoid of SP immunopositive structures, whereas the surrounding hypothalamus contains a dense mesh of SP positive fibers (Fig. 2C).

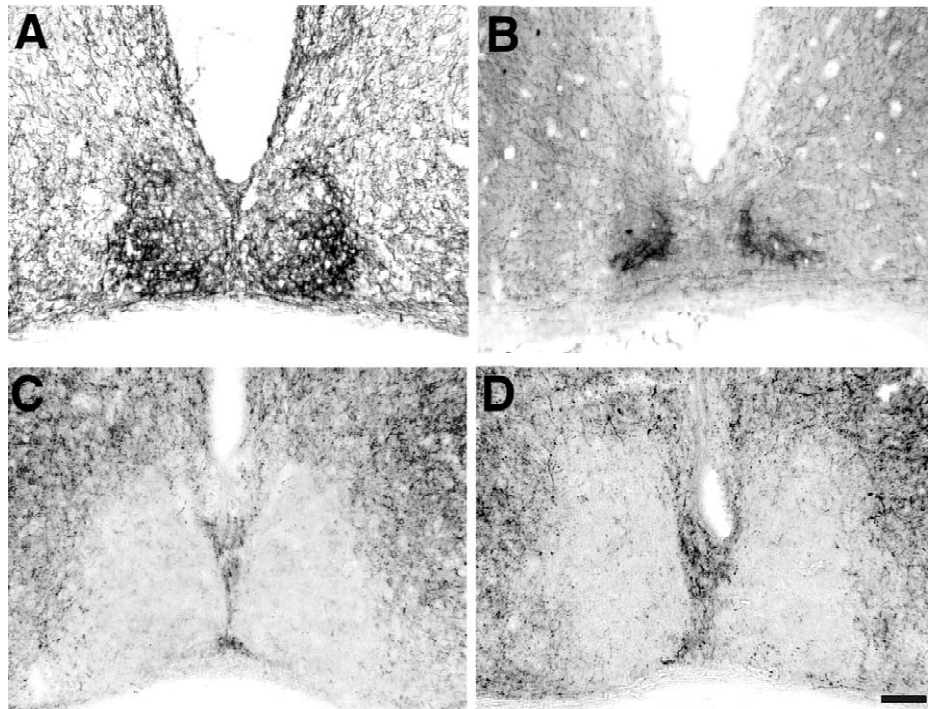


Fig. 2. Organization of the SCN in *Cryptomys*. Distribution of different neuronal markers: Neuropeptide Y (A), serotonin (B), substance P (C), enkephalin (D). Scale: 100  $\mu$ m.

3.1.8. Enkephalin (ENK)

Similar results to the above are observed with the ENK antibody. ENK immunopositive neurons are completely absent from the SCN. The surrounding hypothalamus contains a dense network of ENK positive fibers, which contrasts with the lack of label in the SCN (Fig. 2D).

3.2. Intergeniculate leaflet

In coronal cresyl violet stained sections of the dorsal thalamus, the lateral geniculate complex is located medial to the optic tract. The dorsal lateral geniculate nucleus

(dLGN) is an elongated structure (Fig. 3A). No distinct cellular layers are present, although cells are aligned in 5–6 rows oriented parallel the optic tract. The ventral lateral geniculate nucleus (vLGN; Fig. 3A) is located ventral to the dLGN, and is also distinctly elongate. In between the dLGN and vLGN, the intergeniculate leaflet (IGL) appears as a narrow group of cells (Fig. 3A). Cells in the IGL are more elongate than those of the adjacent geniculate nuclei. Although of very small size, the location and cytoarchitecture of the IGL in *Cryptomys* corresponds to description of this nucleus in other rodents [10]. Retinal afferents to the geniculate are demonstrated by anterograde

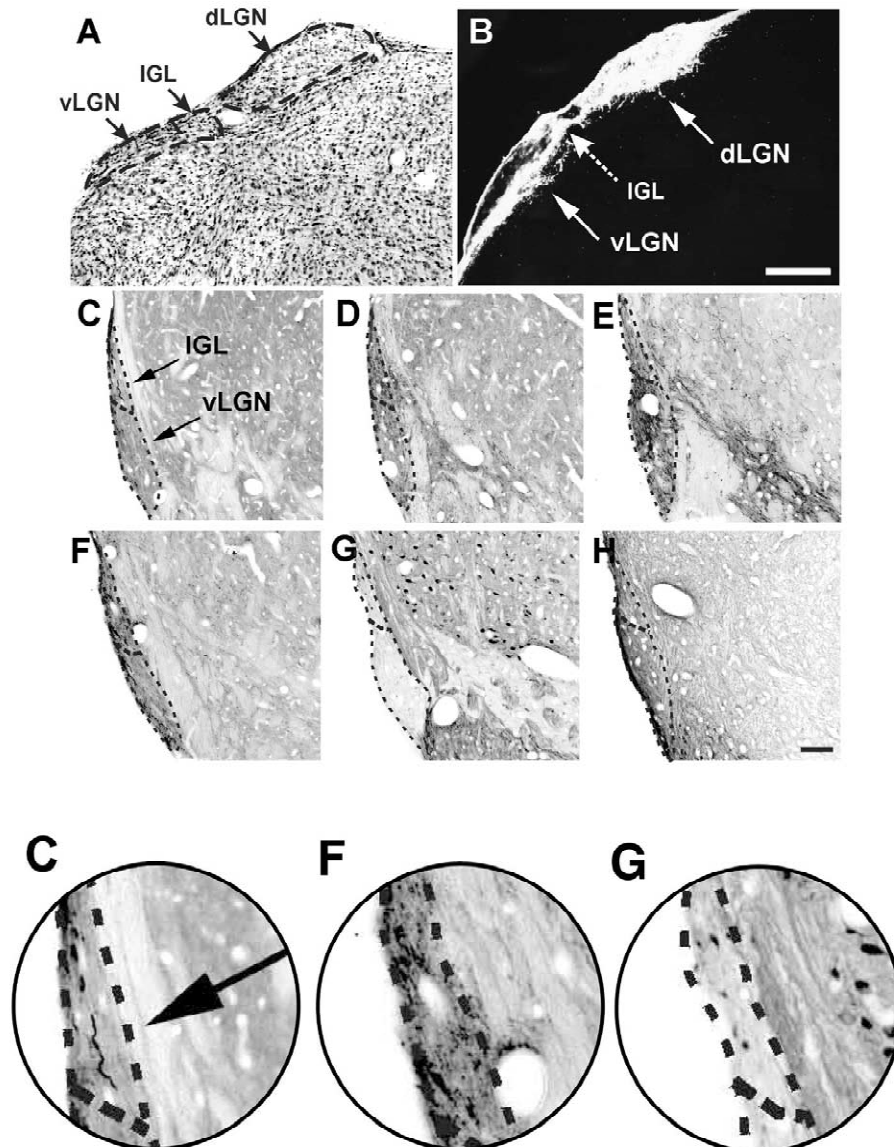


Fig. 3. Organization of the lateral geniculate complex in *Cryptomys*. The cytoarchitecture of the geniculate complex is shown a cresyl violet stained coronal section (A). Retinal afferents to the geniculate complex as demonstrated by anterograde transport of CT-HRP (B). The approximate position of the IGL is shown by the dashed arrow. C–H show the distribution of different neuronal markers of the IGL and vLGN: Neuropeptide Y (C), enkephalin (D), serotonin (E), substance P (F), calbindin (G), parvalbumin (H). High magnification of certain immunopositive labels in the IGL: Neuropeptide Y (C), substance P (F), calbindin (G). dLGN, dorsal lateral geniculate nucleus; IGL, intergeniculate leaflet; vLGN, ventral lateral geniculate nucleus. Scale in B and H: 100  $\mu$ m.

transport of CT–HRP (Fig. 3B). In CT–HRP stained coronal sections, the dLGN and vLGN in *Cryptomys* receives bilateral retinal afferents with a predominance on the contralateral side to the injected eye.

### 3.2.1. Neuropeptide Y (NPY)

Very few immunopositive NPY cells are present in the IGL (about 3 per section). These small neurons are elongate and are oriented in parallel with the dorso–ventral axis of the nucleus. Very few immunopositive NPY fibers are present in the nucleus (Fig. 3C). The dLGN also contains scattered NPY positive cells, which are round in shape, as well as NPY fibers. In contrast, the vLGN only contains some sparse NPY fibers adjacent to the optic tract.

### 3.2.2. Enkephalin (ENK)

ENK immunopositive cells are absent and fibers are sparse in the LGN. The dLGN is devoid of any ENK fibers, whereas the IGL and the adjacent dorsal region of the vLGN, contain a moderate amount of ENK positive fibers (Fig. 3D).

### 3.2.3. Serotonin (5-HT)

The entire geniculate complex contains numerous 5-HT immunopositive fibers. The dLGN and vLGN are particularly rich in 5-HT fibers (Fig. 3E). The IGL contains a moderate amount of 5-HT fibers.

### 3.2.4. Substance P (SP)

The IGL contains a moderately dense plexus of immunoreactive fibers, which is intercalated between the dLGN and vLGN (Fig. 3F). The dLGN contains few SP fibers, mainly located adjacent to the optic tract, whereas SP fibers are diffusely distributed in the vLGN.

### 3.2.5. Calbindin (CAL)

The IGL contains a sparse population of CALB positive cells (Fig. 3G), which are elongate in shape. The dLGN contains sparsely distributed, round CALB positive cells, whereas very few CALB containing cells are observed in the vLGN.

### 3.2.6. Parvalbumin (PARV)

PARV immunopositive cells are completely absent from the entire geniculate complex, although cells containing this calcium binding protein are evident in other adjacent regions, for example some cells in the substantia nigra (Fig. 3H).

## 3.3. Infection of visual structures by PRV-Bartha and PRV-Becker strains

Following intravitreal injection, the neurovirulence of the two strains of PRV differ in *Cryptomys*. Animals infected with the wild type Becker strain did not survive longer than 82 h, whereas animals infected with the Bartha strain survived up to 118 h. Similar observations have been made in other rodents (rat: [11], mouse: [51]). The reduced neurovirulence of the Bartha strain is attributed to the deletion of certain components of the glycoprotein envelope [11,12]. For both strains, the number of infected neurons in structures receiving retinal afferents increases exponentially with post-survival time. In contrast, the pattern of infection by each strain differs in structures of the visual and circadian pathways.

### 3.3.1. Suprachiasmatic nucleus (SCN)

After intraocular injection of the PRV-Becker strain, a few infected neurons (less than 5) are observed in the ipsilateral SCN after 66 h survival. After 82 h, the number of infected neurons slightly increases (35) and cells are observed loosely scattered bilaterally in the nucleus, predominantly on the ipsilateral side (Table 1; Fig. 4A).

Injection of the Bartha strain leads to infected neurons in the SCN as early as 70 h. The number of infected neurons continues to increase significantly reaching a maximum of 2600–2800 cells at 111 and 118 h post survival times. In most cases there is a slight predominance on the ipsilateral side (Table 1). Within the SCN, infected neurons are densely clustered in the ventral region of the nucleus (Fig. 4B).

Table 1

Total number of infected neurons by the PRV-Becker and PRV-Bartha strains on the contralateral ('C') and ipsilateral ('I') sides of different visual structures

Becker	SCN		dLGN		IGL		vLGN		PRT		SC	
	C	I	C	I	C	I	C	I	C	I	C	I
66 h	0	5	0	0	0	0	0	0	5	1	0	0
82 h	12	23	170	4	0	0	6	0	25	13	4	0
Bartha												
70 h	27	3	1	0	0	0	0	0	14	2	0	0
90 h	4	34	0	1	0	0	0	0	15	5	0	0
100 h	206	311	0	2	0	0	0	1	48	31	0	0
111 h	1368	1282	2	27	0	7	0	6	159	41	0	0
118 h	1354	1488	7	16	1	6	2	6	176	25	12	0



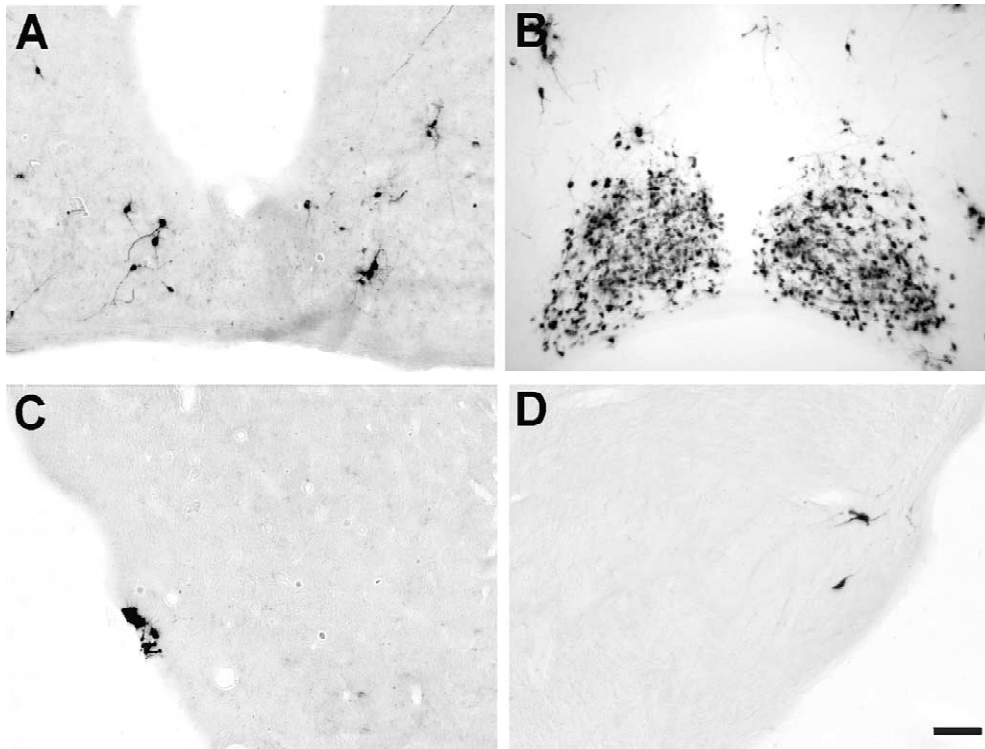


Fig. 4. Distribution of infected neurons in the SCN and IGL/vLGN by the PRV-Becker strain after 82 h post survival (A, SCN; C, IGL) and by the PRV-Bartha after 111 h post survival (B, SCN; D, IGL). Scale: 100  $\mu$ m.

### 3.3.2. Nuclei of the lateral geniculate complex (LGN)

No infected neurons are observed in any region of the geniculate after 66 h survival with the Becker strain. After 82 h, only six cells are observed in the vLGN (Fig. 4C), whereas the number of infected cells has increased dramatically in the dLGN. In both structures, cells are almost exclusively located on the contralateral side (Table 1). Within the dLGN, infected cells occupy a dense focal area (Fig. 5A). The IGL is devoid of infected cells.

Infection by the Bartha strain produces relatively few labeled cells scattered in the dLGN (<30) and vLGN (<8), which are evident only after the longest survival times (111–118 h, Fig. 5B, 4D respectively; see also Table 1). Neurons are mainly located on the ipsilateral side (Table 1). A few labeled cells are also observed in the IGL but only at the longest survival times (Table 1).

### 3.3.3. Pretectum (PRT)

The Becker strain infects few neurons in the PRT at 66 h, and the number of infected neurons increases slightly with the longer survival time of 82 h (<40 cells; Table 1). Infected neurons are mainly located in the olivary pretectal nucleus (OPN) (Fig. 5C), and are predominant contralateral to the injected eye (Table 1).

Infection of pretectal neurons by the Bartha strain begins as early as 70 h survival time, and approximately doubles in number in cases with each additional 10 h survival. Infected neurons are predominantly on the contralateral

side, and as in the case of PRV-Becker are located in the OPN (Table 1, Fig. 5D).

### 3.3.4. Superior colliculus (SC)

Intraocular injection of either the Becker strain or the Bartha strain fails to produce infected neurons in the superior colliculus, except at the longest survival times in each case. At 82 h, only 4 cells are observed in the colliculus with the Becker strain (Fig. 5E), and at 118 h only 12 cells are observed with the Bartha strain, all located contralateral to the injected eye (Table 1).

### 3.3.5. Other structures

Infected neurons were observed in a few additional structures after 82 and 100 h survival times for the Becker and Bartha strains, respectively. Within the hypothalamus, scattered labeled neurons are seen in the lateral hypothalamic region, the paraventricular nucleus, and the periventricular nucleus. All these structures have been shown to receive sparse retinal input in rodents, including subterranean mammals [32]. A few cells are also seen in the deep regions of the superior colliculus and in the periaqueductal gray, as well as in a few diverse thalamic regions. The sparsely infected neurons in these regions are probably the result of transsynaptic transport from primary visual structures. No infected neurons were observed in the accessory optic system, which in subterranean rodents is extremely reduced [17,18].



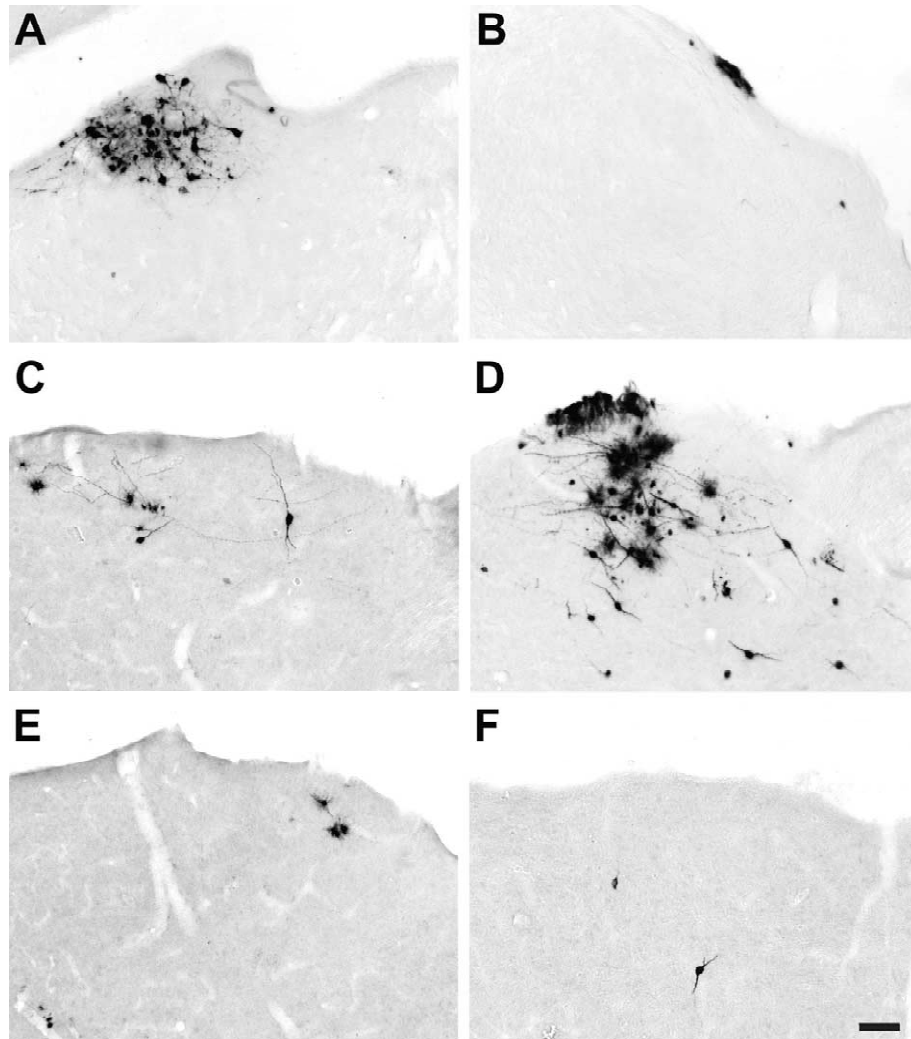


Fig. 5. Distribution of infected neurons by the PRV-Becker strain after 82 h post survival in the dLGN (A), PRT (C), and the SC (E). Distribution of infected neurons by the PRV-Bartha after 111 h post survival in the dLGN (B), PRT (D) and the SC (F). Scale: 100  $\mu$ m.

### 3.3.6. Retinal ganglion cells

No ganglion cells were detected in the contralateral uninjected eye with the Becker strain after 66 and 82 h survival. With the Bartha strain, a distinct subpopulation of infected ganglion cells is observed after 118 h survival.

The total number of labeled ganglion cells in the contralateral retina is 170. These cells are distributed over the entire surface of the retina, with the majority located in the ventral region (Fig. 6A). The temporal, nasal and dorsal quadrants contain 20–30 labeled cells, whereas the ventro lateral quadrant contains nearly 100 labeled ganglion cells.

The morphology of the labeled ganglion cells appears to form a homogeneous population. The soma are slightly oval in shape and range in diameter from 7.70  $\mu$ m to 16.31  $\mu$ m (mean =  $12.70 \pm 1.81$   $\mu$ m,  $n=30$  cells). The ganglion cells possess only two to three primary dendrites, which often extend for some distance from the soma, but have few branches and few varicosities (Fig. 6B,C).

## 4. Discussion

In mammals, daily activity and neuroendocrine rhythms are regulated by the endogenous circadian clock located in the SCN [58]. Neuronal activity and the phase of the endogenous clock are modulated by ambient levels of light via the retinohypothalamic tract [36]. The IGL, which also receives a direct retinal innervations and projects to the SCN via the geniculohypothalamic tract [48] is also an integral component of the circadian system [31,49]. The distribution and physiology of neurotransmitters in the SCN and IGL, as well as their neuronal connections have been widely studied in a number of rodents including the rat [40,65], mouse [16,51], hamster [42], squirrel [57] and blind mole-rat *Spalax* [44]. Based on these studies, the SCN can be divided into two main regions, according to the distribution of neuropeptides, retinal innervations, and afferent and efferent connections. For example in the rat, the dorsal region contains vasopressinergic and somatos-



Fig. 6. Distribution of infected ganglion cells in the entire retina of *Cryptomys* after 118 h post survival (A; scale: 300  $\mu\text{m}$ ). Morphology of the infected ganglion cells (B–C; scale: 30  $\mu\text{m}$ ).

tatin containing neurons, as well as VIP fibers. The ventral region, which receives the retinal afferents, contains mainly VIP and GRP neurons, and fibers immunoreactive for 5-HT, NPY and SP. The characteristic features of these subdivisions are considered to be intimately related to the generation and expression of circadian rhythmicity. Since these features have not been investigated in mammals such as the subterranean species *Cryptomys*, which appear to lack circadian rhythmicity and light mediated entrainment, it is interesting to compare the organization of the circadian system and visual pathways of this species to that of other mammals.

#### 4.1. Organization of the SCN

The distribution of VIP neurons in the ventral region of

the SCN of *Cryptomys* is comparable to that of other rodents. In rodents, immunohistochemical, ultrastructural and physiological studies have shown that this ventral region represents a 'central platform' where information from various sources converges in the SCN. For example, most afferents to the SCN, such as 5-HT fibers from the raphe nucleus, NPY fibers from the IGL, and glutamergic retinal afferents make synaptic contacts on VIP cells [25,26,28]. VIP neurons are essentially implicated in local connections within the ventral region with VIP containing and other cellular populations, in the dorsal region with VP containing neurons, and in adjacent hypothalamus [29]. Intrinsic and extrinsic VIP projection patterns of the SCN are organized in a fashion that suggest VIP neuronal connections are critical in the coupling of the SCN with environmental light–dark cycles, coordination of rhythmic

activity within and between diencephalic cell population [55].

In contrast, VP has been shown to display a distinct endogenous rhythm in the SCN in constant conditions [67]. VP containing neurons represent the most numerous neuropeptidergic population in the nucleus of all rodent studied and the main efferent system of the SCN [9]. VP containing neurons are generally located in the dorsal region [65], whereas, in *Cryptomys*, VP neurons are located in the ventral and medial regions, extending only partially to the dorsal pole of the nucleus.

In *Cryptomys*, the distribution of GRP containing neurons is partially comparable to that of other rodents such as the rat and hamster [65]. GRP cells are located in the ventral part of the SCN in other rodents, whereas in *Cryptomys* the distribution also extends into the central region of the nucleus. The RHT terminates make synaptic contacts with GRP neurons in rat [60], indicate that GRP neurons, like VIP neurons, receive a visual input, and may be critical in the entrainment of the SCN to the environmental light–dark cycle.

In *Cryptomys*, the calcium binding protein, CALB, is distributed throughout the entire SCN. A similar distribution has been described in the marmoset [20] and in the mouse [1], although in other species CALB neurons are located at the periphery (rat [15]) or the central region of the nucleus (human [35]; rat [54]). The distribution of the calcium binding protein into the SCN was variable in mammals. The precise role of CALB in intracellular calcium binding, neuronal excitability, and signal transduction is not fully understood. Nevertheless, some studies have shown that the CALB neuronal population of the SCN is essential for maintaining circadian rhythmicity in tissue transplants to SCN lesioned animals [56].

Both NPY and 5-HT represent important afferent inputs to the SCN and are implicated in numerous aspects of the regulation and control of circadian rhythms [8,42]. In *Cryptomys*, the NPY fibers plexus in the SCN is moderately dense compared to other rodents, although the distribution slightly differs. Indeed, NPY fibers are located in the ventral and lateral regions of the SCN, whereas in most other rodents NPY is mainly restricted to the ventral region [16,65]. The presence of NPY containing fibers in the SCN suggests the presence of a geniculohypothalamic tract in *Cryptomys*, although the number of NPY neurons in the IGL is relatively reduced.

The 5-HT innervations of the SCN by the raphe nucleus are one of the densest of all brain regions [26]. The distribution of 5-HT fibers in *Cryptomys* is similar to that of other rodents, and overlaps the distribution of VIP cells and NPY fibers [65].

In summary, the distribution of neurotransmitters in the SCN of *Cryptomys* allows a subdivision of the nucleus into two main regions as in other rodents, but a number of differences are seen in the distribution of certain neurotransmitters. The ventral region contains, in particular, a VIP neuronal population and afferent NPY and 5-HT fibers

as well retinal afferents, but also VP neurons. The dorsal region contains VIP fibers and a VP neuronal population, which only partially extends in this region. Contrary to typical rodent pattern of organization, the presence in the ventral region of partially overlapping populations of both VIP and VP neurons, as well as the partial segregation of VIP neurons and 5-HT fibers, compared to the NPY fibers may be correlated with the apparent absence of light entrainment of activity and lack of endogenous rhythmicity in *Cryptomys*. This hypothesis must be confirmed by other cellular and behavioral investigations.

It must be emphasized that in other rhythmic mammals, some of these differences have also been observed, such as marsupials, in which VIP and VP neurons are located in the same region of the SCN [13]. In the same way, a recent paper shows that NPY fibers were detected in the ventral portion of the marmoset SCN although 5-HT fibers were found mostly in central and dorsal areas [14].

#### 4.2. Organization of the IGL

In the blind mole-rat, *Spalax*, the IGL could not be distinguished either from cytoarchitecture or from tracing of retinal projections [17]. This is partly related to the reduced size of the entire geniculate complex in the species. In *Cryptomys*, although this reduction is not as significant, the identification of the IGL based on cresyl violet stained sections alone is difficult. The presence of NPY cells as well as ENK and SP fibers in the region located between the dLGN and the vLGN allows identification of this structure.

The IGL in *Cryptomys* is a small triangular shaped group of cells intercalated between the dLGN and vLGN. As in other rodents, the IGL contains both elongated cells and fibers immunoreactive for NPY [40]. The dLGN in *Cryptomys* also contains NPY positive fibers and scattered cells, but these are of different morphology from those in the IGL, whereas the vLGN contains only NPY fibers. This difference facilitates the distinction between IGL and other geniculate nuclei. In other rodents, such as the NPY cells are absent from the dLGN and scarce in the vLGN [40]. In species like the cat, however, numerous NPY cells in the vLGN render the distinction with the IGL more difficult. The NPY cells of the IGL are at the origin of the GHT in rodents [42,43]. The presence of NPY cells in this structure in *Cryptomys*, although few in number, as well as the presence of NPY fibers in the ventral region of the SCN, argues in favor of the existence of this pathway in the mole-rat.

The distribution of SP positive fibers in the lateral geniculate complex is similar to that described in the rat and hamster [40]. In these species SP fibers fill the entire rostro–caudal extent of the IGL. In *Cryptomys*, scattered SP fibers are present in the both the vLGN and the dLGN, whereas the IGL appears as a compact nucleus densely filled with SP positive fibers at the dorsal extremity of the vLGN. Although SP positive neurons have been observed

in the IGL of some species [61], we have not made similar observations in the mole rat.

We have been unable to identify any ENK containing neurons in the IGL of *Cryptomys*, in contrast to observations in other rodents [40]. In the mole rat, ENK positive cells are absent from all parts of the geniculate complex, and only the vLGN show a significant density of ENK positive fibers. In other rodents, ENK cells project either to the contralateral IGL (rat [10]), or to the SCN (hamster [42,43]). These projections may, thus, be lacking in *Cryptomys*.

The calcium binding protein PARV, has also been shown to be an appropriate marker of the IGL, since in other rodents, PARV positive cells are present in all parts of the LGN, except for the IGL [40]. In *Cryptomys*, this was not the case, and PARV is absent from the entire geniculate complex. In contrast, CALB positive cells are located in the IGL, and show an elongate morphology, which distinguishes them from those in the dLGN.

In summary, the IGL in *Cryptomys* is distinguishable from combined cytoarchitectural and neuropeptidergic features, although the size of the nucleus (as for the remainder of the geniculate complex) is highly reduced. It is unknown whether this structure plays a role in either photic or non-photoc mediation of locomotor behavior in this species.

#### 4.3. Infection of retinal pathways by pseudorabies virus

The tracing of retinal projections using the neurotropic infectious properties of the two strains of pseudorabies virus show distinctly different patterns of infection in the visual and circadian pathways. The wild type PRV-Becker strain primarily infects neurons in the dLGN, whereas the attenuated PRV-Bartha strain primarily leads to infection of neurons in the SCN. These different patterns of infection argue in favor of a fundamental dichotomy between the circadian and other visual pathways. This segregation has been suggested by several anatomical [11,34,47,51] electrophysiological [36] and behavioral studies [45]. The results also confirm the conservation of the circadian and visual pathways in *Cryptomys*.

##### 4.3.1. Infection by the PRV-Becker strain

Following a survival time of 66 h, hardly any neuronal infection by PRV-Becker is visible in the visual system virus of *Cryptomys*. After 82 h survival after intraocular injection, infected neurons are evident in several structures innervated by the retina. The total number of infected neurons is less than 260, which is nearly 1000 times less than the number of neurons infected by PRV-Becker in the mouse at an equivalent survival time [51]. This reduction is related to the relative regression in size of the retina and of visual structures in *Cryptomys*, which similar to, but of lesser magnitude than that observed in the blind mole rat, *Spalax* [17,18].

The dLGN is the main site of viral infection, accounting

for almost 70% of all infected neurons. Both the PRT (mainly the OPN) and the SCN contain about 13–14% of the infected neurons. Very few neurons are seen in the vLGN and superior colliculus. No infected neuron could be distinguished in the IGL. The absence or extremely scarcity of neurons in certain structures is not surprising considering the degree of anatomical regression of visual structures. This is particularly evident concerning the IGL, which is very difficult to distinguish in *Cryptomys*, especially in these tracing experiments where other markers were lacking. In contrast, the number of infected neurons in the SCN after a survival period of 70–80 h is very similar to that of other rodents: In the rat, about 50 neurons [11], and in the mouse, about 30 neurons [51]. However, in these latter species of murine rodents, there is abundant infection of visual structures such as the PRT, vLGN and especially the colliculus superior at equivalent survival times. For example, the colliculus in *Cryptomys* is almost devoid of labeled neurons, whereas in the mouse this structure contains more than 7000 neurons after 80 h survival. Despite the reduced number of infected neurons, the general pattern of infection in *Cryptomys* is similar to results in the rat [11] and the mouse [51].

It is also interesting to note that in the SCN infected neurons are mainly located ipsilateral to the injected eye, whereas in other structures, the contralateral side mainly contains infected neurons. In the mouse as well, labeled neurons are mainly observed on the ipsilateral side [51]. The results agree with our retinal tracing experiments in *Cryptomys* using cholera toxin conjugated with HRP, which show that the label is mainly located on the ipsilateral side in the SCN, and on the contralateral side in other visual structures (this study and personal observations).

##### 4.3.2. Infection by the PRV-Bartha strain

At the earliest survival times (70–90 h) infection of visual structures is very reduced, and is roughly similar to the temporal course of infection with the PRV-Becker Strain. However, at longer survival times, the infection rapidly increases to reach a peak at 111–118 h. In particular the SCN contains more than 90% of all the infected neurons in retinally innervated structures. The total number of infected neurons is even higher in *Cryptomys* than in the mouse [51] where we have also done a careful quantitative study, but appears to be in the range of that observed in the rat by Card et al. [11]. The bilateral distribution of infected neurons in the SCN shows a slight ipsilateral predominance in most cases.

The only other structure showing a significant number of infected neurons is the PRT (6.4%). The number and proportion of label is far inferior to that observed in the mouse and rat [11,51]. However, as in the mouse, infected neurons in the PRT are located almost exclusively in the OPN, contralateral to the injection.

Other structures (IGL, vLGN, dLGN, SC) account for less than 2% of the infected neurons. This highly contrasts

with results in other rodents, in particular for the IGL in which the neuronal infection is quantitatively and qualitatively distinctive. As suggested above, we attribute this reduced infection in *Cryptomys* to the significant reduction of the geniculate complex, and of the superior colliculus in the mole rat as compared to other rodents. The limited number and delayed appearance of the infection in these structures (in general after 111 h), as well as the bilateral distribution, suggests that infected neurons are mainly the result of a retrograde transneuronal transport. For example, the few neurons present in the dLGN, vLGN and IGL are located on the ipsilateral side, which may be related to transneuronal infection from the SCN, whereas the few neurons in the colliculus are located on the contralateral side, which may be related to transneuronal infection from the PRT.

These observations agree with a recent paper of Pickard et al. [50] showing that the infection of retinorecipient structures such as the SCN, IGL and PRT in rat, after intravitreal PRV Bartha injection results from retrograde transsynaptic transport via autonomic afferents to the eye and not by anterograde transport via the optic nerve. PRV Bartha should be considered a transsynaptic marker that travels exclusively in a retrograde direction in the central nervous system.

#### 4.4. Infection of retinal ganglion cells by PRV-Bartha

The retina contralateral to the injected eye in the case of 118 h survival contained about 170 infected ganglion cells which represents about 5.0% of the total ganglion cell population [23]. The ganglion cells show a relatively homogeneous distribution in the retina, but with a higher concentration in the ventral region. This may correspond to the fact that any encounter with light in the subterranean mammals during opening of the underground galleries, would be from a dorsally located source impinging mainly on the ventral region of the retina.

Most ganglion cells form a morphologically homogeneous population. Many cells are characterized by a small to medium sized soma, with two to three long primary dendrites with few branches. After 118 h survival, the number of infected neurons by PRV-Bartha in the SCN is about 10 times more than the number of infected neurons in PRT and other structures. Consequently, most ganglion cells infected by retrograde transport of the Bartha strain project principally in the SCN and resemble the retinohypothalamic ganglion cells described in the sheep [19], rat [41], hamster [46] and mouse [51].

#### Acknowledgements

We would like to thank Christel Merrouche for help with histology, and Ghislaine Claine for care of the animals. The research was funded by grants from Human

frontier (RG95/68), NATO (#950334), ENP (#185), and BIOMED2 (PL/962327).

#### References

- [1] E.E. Abrahamson, R.Y. Moore, Suprachiasmatic nucleus in the mouse: retinal innervation, intrinsic organization and efferent projections, *Brain Res.* 916 (2001) 172–191.
- [2] A. Bartha, Experimental reduction of virulence of Aujeszky's diseases virus, *Maggi. Alatorv. Lapja. cell* (1961) 42–45.
- [3] C.H. Becker, Zur primären schädigung vegetativer ganglien nach infektion mit dem herpes suis virus bei verschiedenen tierarten, *Eperiencia* 23 (1967) 209–217.
- [4] N.C. Bennett, The social structure and reproductive biology of the common mole rat, *Cryptomys h. hottentotus* and remarks on the trends in reproduction and sociality in the family Bathyergidae, *J. Zool. Lond.* 219 (1989) 45–59.
- [5] N.C. Bennett, The locomotor activity patterns of a functionally complete colony of *Cryptomys hottentotus hottentotus* (Rodentia: Bathyergidae), *J. Zool. Lond.* 228 (1992) 435–443.
- [6] A.D. Brideau, M.G. Eldridge, L.W. Enquist, Directional transneuronal infection by pseudorabies virus is dependent on an acidic internalization motif in the Us9 cytoplasmic tail, *J. Virol.* 74 (2000) 4549–4561.
- [7] G. Bronchti, R. Rado, J. Terkel, Z. Wollberg, Retinal projections in the blind mole rat: a WGA-HPR tracing study of a natural degeneration, *Dev. Brain Res.* 58 (1991) 159–170.
- [8] F.R. Cagampang, S.T. Inouye, Diurnal and circadian changes of serotonin in the suprachiasmatic nuclei: regulation by light and an endogenous pacemaker, *Brain Res.* 639 (1994) 175–179.
- [9] J.P. Card, S. Fitzpatrick-McElligott, I. Gozes, F. Baldino, Localization of vasopressin-, vasoactive intestinal polypeptide-, peptide histidine isoleucine- and somatostatin-mRNA in rat suprachiasmatic nucleus, *Cell Tissue Res.* 252 (1988) 307–315.
- [10] J.P. Card, R.W. Moore, Organization of lateral geniculate–hypothalamic connections in the rat, *J. Comp. Neurol.* 284 (1989) 135–147.
- [11] J.P. Card, M.E. Whealy, A.K. Robbins, R.Y. Moore, L.W. Enquist, Two alpha-Herpes virus strains are transported differentially in the rodent visual system, *Neuron* 6 (1991) 957–969.
- [12] J.P. Card, L.W. Enquist, Neurovirulence of pseudorabies virus, *Crit. Rev. Neurobiol.* 9 (1995) 137–162.
- [13] V.M. Cassone, J.C. Speh, J.P. Card, R.Y. Moore, Comparative anatomy of the mammalian hypothalamic suprachiasmatic nucleus, *J. Biol. Rhythms* 3 (1988) 71–91.
- [14] J.S. Cavalcante, A.S. Alves, M.S.M.O. Costa, L.R.G. Britto, Differential distribution of afferents containing serotonin and neuropeptide Y within the marmoset suprachiasmatic nucleus, *Brain Res.* 927 (2002) 200–203.
- [15] M.R. Celio, Calbindin D-28k and parvalbumin in the rat nervous system, *Neuroscience* 35 (1990) 375–475.
- [16] C.S. Colwell, R.G. Foster, Photic regulation of Fos-like immunoreactivity in the suprachiasmatic nucleus of the mouse, *J. Comp. Neurol.* 324 (1992) 135–142.
- [17] H.M. Cooper, M. Herbin, E. Nevo, Visual system of a naturally microphthalmic mammal: the blind mole rat, *Spalax ehrenbergi*, *J. Comp. Neurol.* 328 (1993) 313–350.
- [18] H.M. Cooper, M. Herbin, E. Nevo, Ocular regression conceals adaptive progression of the visual system in a blind subterranean mammal, *Nature* 361 (1993) 156–159.
- [19] H.M. Cooper, A. Tessonnaud, A. Caldani, A. Locatelli, S. Richard, M.C. Viguier-Martinez, Morphology and distribution of retinal ganglion cells projecting to the suprachiasmatic nucleus in the sheep, *Am. Soc. Neurosci. Abstr.* 19 (1993) 701.11.
- [20] M.S. Costa, L.R. Britto, Calbindin immunoreactivity delineates the

- circadian visual centers of the brain of the common marmoset (*Callithrix jacchus*), Brain Res. Bull. 43 (1997) 369–373.
- [21] G. Eloff, Functional and structural degeneration of the eye of the south African rodent mole, *Cryptomysbigalkei* and *Bathyergus maritimus*, S. Afr. J. Sci. 54 (1958) 292–302.
- [22] A.R. Gibson, D.I. Hansma, J.C. Houk, F.R. Robinson, a sensitive low artifact TMB procedure for the demonstration of WGA-HRP in the CNS, Brain Res. 298 (1984) 235–241.
- [23] M. Herbin, Etude Comparative des Modifications Anatomo-fonctionnelles du Système Visuel Primaire chez les Mammifères Microphthalmes, Ph.D., University of Paris VII, 1993.
- [24] G.C. Hickman, Locomotory activity of captive *Cryptomys hottentotus* (Mammalia: Bathiergidae), a fossorial rodent, J. Zool. Lond. 192 (1980) 225–235.
- [25] S. Hisano, M. Chikamori-Aoyama, S. Katoh, Y. Kagotani, S. Daikoku, K. Chihara, Suprachiasmatic nucleus neurons immunoreactive for vasoactive intestinal polypeptide have synaptic contacts with axons immunoreactive for neuropeptide Y: an immunoelectron microscopic study in the rat, Neurosci. Lett. 88 (1988) 145–150.
- [26] S. Hisano, M. Chikamori-Aoyama, S. Katoh, M. Maegawa, S. Daikoku, Immunohistochemical evidence of serotonergic regulation of vasoactive intestinal polypeptide (VIP) in the rat suprachiasmatic nucleus, Histochemistry 86 (1988) 573–578.
- [27] P.J. Husak, T. Kuo, L.W. Enquist, Pseudorabies virus membrane proteins gI and gE facilitate anterograde spread of infection in projection-specific neurons in the rat, J. Virol. 74 (2000) 10975–10983.
- [28] Y. Ibata, T. Takahashi, H. Okamura et al., Vasoactive intestinal peptide (VIP) like immunoreactive neurons located in the rat suprachiasmatic nucleus receive a direct retinal projection, Neurosci. Lett. 97 (1989) 1–5.
- [29] Y. Ibata, M. Tanaka, Y. Ichitani, Y. Takahashi, H. Okamura, Neuronal interaction between VIP and vasopressin neurones in the rat suprachiasmatic nucleus, Neuroreport 4 (1993) 128–130.
- [30] S.T. Inouye, S. Shibata, Neurochemical organization of circadian rhythm in the suprachiasmatic nucleus, Neurosci. Res. 20 (1994) 109–130.
- [31] R.F. Johnson, R.Y. Moore, L.P. Morin, Lateral geniculate lesions alter circadian activity rhythms in the hamster, Brain Res. Bull. 22 (1989) 411–422.
- [32] M. Kudo, M. Yamamoto, Y. Nakamura, Suprachiasmatic nucleus and retinohypothalamic projections in moles, Brain Behav. Evol. 38 (1991) 332–338.
- [33] H.G. Kuypers, G. Ugolini, Viruses as transneuronal tracers, Trends Neurosci. 13 (1990) 71–75.
- [34] M. Magnin, H.M. Cooper, G. Mick, Retinohypothalamic pathway: a breach in the law of Newton–Müller–Gudden?, Brain Res. 488 (1989) 390–397.
- [35] J.K. Mai, O. Kedziora, L. Teckhaus, M.V. Sofroniew, Evidence for subdivisions in the human suprachiasmatic nucleus, J. Comp. Neurol. 305 (1991) 508–525.
- [36] J.H. Meijer, W.J. Rietveld, Neurophysiology of the suprachiasmatic circadian pacemaker in rodents, Physiol. Rev. 69 (1989) 671–707.
- [37] M.M. Mesulam, Tetramethyl benzidine for horseradish peroxidase neurohistochemistry: a non-carcinogenic blue reaction product with superior sensitivity for visualizing neural afferents and efferents, J. Histochem. Cytochem. 26 (1978) 106–117.
- [38] M. Möller, J.D. Mikkelsen, J. Fahrenkrug, H.W. Korf, The presence of vasoactive intestinal polypeptide (VIP)-like-immunoreactive nerve fibres and VIP receptors in the pineal gland of the Mongolian gerbil (*Meriones unguiculatus*). An immunohistochemical and receptor–autoradiographic study, Cell Tissue Res. 241 (1985) 333–340.
- [39] R.Y. Moore, Organization of the primate circadian system, J. Biol. Rhythm 8 (1993) S3–S9.
- [40] R.Y. Moore, J.P. Card, Intergeniculate leaflet. An anatomically and functionally distinct subdivision of the lateral geniculate complex, J. Comp. Neurol. 344 (1994) 403–430.
- [41] R.Y. Moore, J.C. Speh, J.P. Card, The retinohypothalamic tract originates from a distinct subset of retinal ganglion cells, J. Comp. Neurol. 352 (1995) 351–366.
- [42] L.P. Morin, J. Blanchard, R.Y. Moore, Intergeniculate leaflet and suprachiasmatic nucleus organization and connections in the golden hamster, Vis. Neurosci. 8 (1992) 219–230.
- [43] L.P. Morin, J. Blanchard, Neuropeptide Y and enkephalin immunoreactivity in retinorecipient nuclei of the hamster pretectum and thalamus, Vis. Neurosci. 14 (1997) 765–777.
- [44] J. Negroni, E. Nevo, H.M. Cooper, Neuropeptidergic organization of the suprachiasmatic nucleus in the blind mole rat (*Spalax ehrenbergi*), Brain Res. Bull. 44 (1997) 633–639.
- [45] D.E. Nelson, J.S. Takahashi, Sensitivity and integration in a visual pathway for circadian entrainment in the hamster (*Mesocricetus auratus*), J. Physiol. 439 (1991) 115–145.
- [46] G.E. Pickard, Morphological characteristics of retinal ganglion cells projecting to the suprachiasmatic nucleus: a horseradish peroxidase study, Brain Res. 183 (1980) 458–465.
- [47] G.E. Pickard, A.-J. Silverman, Direct retinal projections to the hypothalamus, piriform cortex and accessory optic nuclei in the golden hamster as demonstrated by a sensitive anterograde horseradish peroxidase technique, J. Comp. Neurol. 196 (1981) 155–172.
- [48] G.E. Pickard, Bifurcating axons of retinal ganglion cells terminate in the hypothalamic suprachiasmatic nucleus and the intergeniculate leaflet of the thalamus, Neurosci. Lett. 55 (1985) 211–217.
- [49] G.E. Pickard, Entrainment of the circadian rhythm of wheel-running activity is phase shifted by ablation of the intergeniculate leaflet, Brain Res. 494 (1989) 151–154.
- [50] G.E. Pickard, C.A. Smeraski, C.C. Tomlinson et al., Intravitreal injection of the attenuated pseudorabies virus PRV Bartha results in infection of the hamster suprachiasmatic nucleus only by retrograde transsynaptic transport via autonomic circuits, J. Neurosci. 22 (2002) 2701–2710.
- [51] I. Provencio, H.M. Cooper, R.G. Foster, Retinal projections in mice with inherited retinal degeneration: implications for circadian photo-entrainment, J. Comp. Neurol. 395 (1998) 417–439.
- [52] R. Rado, H. Gev, J. Terkel, The role of light in entraining mole rats' circadian rhythms, Israel J. Zool. 35 (1988) 105–106.
- [53] R. Rado, J. Terkel, Circadian activity of the blind mole rats *Spalax ehrenbergi* monitored by radio-telemetry in seminatural and natural conditions, in: E. Spanier, Y. Steinberger, M. Luria (Eds.), Environmental Quality and Ecosystem Stability, Vol. B, ISEEQS, Jerusalem, 1989, pp. 391–400.
- [54] J.H. Roger, A. Résibois, Calretinin and Calbindin-D28k in rat brain: patterns of partial co-localization, Neuroscience 51 (1992) 843–865.
- [55] K. Shinohara, K. Tominaga, Y. Isobe, S.I. Inouye, Photic regulation of peptides located in the ventrolateral subdivision of the suprachiasmatic nucleus of the rat—Daily variations of vasoactive intestinal polypeptide, gastrin-releasing peptide, and neuropeptide-Y, J. Neurosci. 13 (1993) 793–800.
- [56] R. Silver, M.T. Romero, H.R. Besmer, R. Leak, J.M. Nunez, J. LeSauter, Calbindin-D28K cells in the hamster SCN express light-induced Fos, Neuroreport 7 (1996) 1224–1228.
- [57] L. Smale, J. Blanchard, R.Y. Moore, L.P. Morin, Immunocytochemical characterization of the suprachiasmatic nucleus and the intergeniculate leaflet in the diurnal ground squirrel, *Spermophilus lateralis*, Brain Res. 563 (1991) 77–86.
- [58] F.K. Stephan, A. Nunez, Elimination of circadian rhythms in drinking, activity, sleep and temperature by isolation of the suprachiasmatic nuclei, Behav. Biol. 20 (1977) 1–16.
- [59] P.L. Strick, J.P. Card, Transneuronal mapping of neuronal circuits with alpha herpesviruses, in: J.P. Bolam. (Ed.), Experimental Neuroanatomy, A Practical Approach, 1992.
- [60] K. Takatsuji, M. Tohyama, The organization of the rat lateral geniculate body by immunohistochemical analysis of neuroactive substances, Brain Res. 480 (1989) 198–209.
- [61] M. Tanaka, S. Hayashi, Y. Tamada et al., Direct retinal projections

- to GRP neurons in the suprachiasmatic nucleus of the rat, *Neuroreport* 8 (1997) 2187–2191.
- [62] A. Tessoneaud, H.M. Cooper, M. Caldani, A. Locatelli, M.-C. Viguier-Martinez, The suprachiasmatic nucleus in the sheep (*Ovis aries*): retinal projections and cytoarchitectural organization, *Cell Tissue Res.* 278 (1994) 65–84.
- [63] I. Tobler, M. Herrmann, H.M. Cooper, J. Negroni, E. Nevo, P. Aschermann, Rest-activity rhythm of the blind mole rat *Spalax ehrenbergi* under different lighting conditions, *Behav. Brain Res.* 96 (1998) 173–183.
- [64] M.J. Tomishima, L.W. Enquist, A conserved  $\alpha$ -herpesvirus protein necessary for axonal localization of viral membrane proteins, *J. Cell Biol.* 154 (2001) 741–752.
- [65] A.N. van den Pol, K.L. Tsujimoto, Neurotransmitters of the hypothalamic suprachiasmatic nucleus: immunocytochemical analysis of 25 neuronal antigens, *Neuroscience* 15 (1985) 1049–1086.
- [66] P. Vuillez, M. Herbin, H.M. Cooper, E. Nevo, P. Pevet, Photic induction of Fos immunoreactivity in the suprachiasmatic nuclei of the blind mole rat (*Spalax ehrenbergi*), *Brain Res.* 654 (1994) 81–84.
- [67] K.S. Yamase, K. Takahashi, K. Nomura, M. Haruta, S. Kawashima, Circadian changes in arginin vasopressin level in the suprachiasmatic nuclei in the rat, *Neurosci. Lett.* 130 (1991) 255–258.
- [68] L. Zamboni, L. de Martino, Buffered picric acid formaldehyde: a new rapid fixative for electron microscopy, *J. Cell. Biol.* 35 (1967) 148A.